

ChemComm

Accepted Manuscript



This is an *Accepted Manuscript*, which has been through the Royal Society of Chemistry peer review process and has been accepted for publication.

Accepted Manuscripts are published online shortly after acceptance, before technical editing, formatting and proof reading. Using this free service, authors can make their results available to the community, in citable form, before we publish the edited article. We will replace this *Accepted Manuscript* with the edited and formatted *Advance Article* as soon as it is available.

You can find more information about *Accepted Manuscripts* in the [Information for Authors](#).

Please note that technical editing may introduce minor changes to the text and/or graphics, which may alter content. The journal's standard [Terms & Conditions](#) and the [Ethical guidelines](#) still apply. In no event shall the Royal Society of Chemistry be held responsible for any errors or omissions in this *Accepted Manuscript* or any consequences arising from the use of any information it contains.

COMMUNICATION

Compositional Dependent Activity of Cu-Pt Nanocrystals for Electrochemical Reduction of CO₂

Cite this: DOI: 10.1039/x0xx00000x

Xin Guo, Yuxia Zhang, Chen Deng, Xinyuan Li, Yifei Xue, Yi-Ming Yan, and Kening Sun**

Received 00th January 2012,

Accepted 00th January 2012

DOI: 10.1039/x0xx00000x

www.rsc.org/

The Cu-Pt nanocrystals (NCs) samples with concisely controlled atom ratio (Cu : Pt) are prepared by a facile strategy. We demonstrate that Cu-Pt (3:1) NCs exhibits the highest activity and faradaic efficiency in the CO₂ electroreduction reaction among all the as-prepared samples.

The ever-increasing consumption of fossil fuels has accelerated the depletion of natural resources and led to overproduction of carbon dioxide as greenhouse gas.^[1-3] In the past decades, different technologies have been proposed to reduce the emission of CO₂. Among these technologies, conversion of CO₂ into useful low-carbon fuels, such as CO, CH₄, HCOOH, CH₃OH, represents an attracting technology because that it offers a potential way to recycle CO₂ into valuable products for energy needs or for industrial applications.^[4-8] In particular, the electrochemical reduction of CO₂ has drawn extensive attention, as the reaction proceeds cleanly by utilizing sustainable energy (such as wind, solar and hydro).^[9-11] Unfortunately, this avenue is greatly inhibited by the lack of efficient catalysts, which should ideally possess sufficiently low overpotentials and high current densities to achieve high energetic efficiency. Therefore, exploring new electrocatalyst that efficiently reduce CO₂ into liquid fuels, especially in mild conditions, is extremely important.

Researchers have demonstrated that copper is the most promising candidate among pure metals due to its unique ability to catalyze the reduction of CO₂ to form hydrocarbons.^[12] However, the efficiency of Cu based catalysts is largely limited by the large overpotential (> 0.7 V) required for CO₂ reduction to outcompete H₂O reduction.^[13,14] Also, both the selectivity towards the reduction products and the durability of the Cu-based catalysts should be substantially improved before meeting the requirements of practical applications.^[15-17] Moreover, the mechanism of CO₂ reduction on Cu electrodes is complicated and the exactly reaction path is controversy.^[18,19] Despite tremendous experimental efforts and computational calculations^[20-23], the performance of Cu electrocatalyst for CO₂ reduction remains unsatisfied. Recently, Cu-based alloys were reported to possess improved faradaic efficiencies for CO₂ reduction compared to both parent metals. It was found that even small additions of Au (10%) could completely suppress hydrocarbon formation, giving rise instead to highly selective

formation of CO.^[24] On the other hand, the activity of the Cu-based catalysts was reported to strongly depend on their structure and morphology.^[25,26] For example, compared with polycrystalline Cu, nanostructured Cu was demonstrated to possess much higher activity and better selectivity, whereas the major product was ethylene and methane.^[27] The enhanced performance was attributed to the large surface areas and unique structural properties of nanostructured Cu catalysts. More recently, several Cu-based bimetallic nanocrystals (NCs) appear as novel CO₂ electrocatalysts due to their remarkable chemical and physical properties. To this end, Cu-noble metal (such as Au, Pt, Fe, Ag) alloy NCs should be ideal candidates because of their easy preparation and desirable performance.^[22,24,28,29] For instance, Au₃Cu nanocrystals (NCs) have been successfully prepared and exhibited significantly enhanced catalytic activity in the CO₂ electroreduction reaction, compared with monometallic Au nanocrystals. Jin et al. found that the CO₂ reduction current density on the Au₃Cu NCs electrode decreased with an increase of the mass of Au precursor.^[30] Moreover, Pt-supported Cu overlayers were investigated for their catalytic activity and selectivity of CO₂ electroreduction. It was found hydrocarbon production was dependent on the Cu layer thickness.^[27]

Cu-Pt alloy NCs has been previously prepared and used for a variety of applications, such as methanol or formic acid electro-oxidation,^[31-35] heterogeneous NO_x reduction,^[36] CO oxidation^[37] and oxygen reduction reactions.^[38,39] However, as far as we know, Cu-Pt NCs have been rarely investigated as catalysts for electrochemical reduction of CO₂, especially in mild conditions, such as 0.5 M KHCO₃ (pH 7.3) at room temperature. Herein, we report the preparation of monodisperse Cu-Pt NCs by using a co-reduction strategy. With this synthetic method, uniformly distribution of NCs can be realized and atom ratio of Pt and Cu can be concisely controlled. Correspondingly, the Cu-Pt NCs samples show compositional dependent activity towards electrochemical reduction of CO₂. We discover that the sample of Cu-Pt (3:1) NCs exhibits the highest activity and faradaic efficiency as efficient electrocatalyst for CO₂ reduction in 0.5 M KHCO₃ at room temperature. Based on the analysis, we present a plausible mechanism to understand the compositional dependent activity of Cu-Pt NCs.

The Cu-Pt NCs were prepared according to a modified procedures described by Fang et al.^[34] The Cu-Pt NCs prepared with

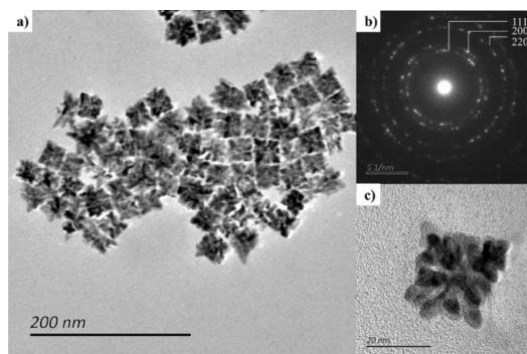


Fig. 1 a) Low magnification TEM image of the overall morphology of Cu-Pt NCs. b) TEM selected-area electron diffraction pattern of the Cu-Pt NCs. c) High-resolution TEM image of a selected Cu-Pt NCs.

different amounts of the Cu precursor and Pt precursor are given as Cu-Pt-1# (1:2), Cu-Pt-2# (1:1), Cu-Pt-3# (2:1), Cu-Pt-4# (3:1) and Cu-Pt-5# (5:1). Fig. 1a shows a typical transmission electron microscopic (TEM) image, displaying the overall morphology of the Cu-Pt-2# (1:1). The sample consists of 24.0 ± 1.0 nm (side length) Cu-Pt NCs. A TEM diffraction pattern of the Cu-Pt NCs (Fig. 1b) indicates a high crystallinity of these NCs (see below). Fig. 1c depicts the high-magnification TEM image of a single Cu-Pt NCs, which reveals that the NCs are composed of many small nanoparticles. Moreover, the Cu weight ratios in the Cu-Pt NCs were extensively identified by inductively coupled plasma atomic emission spectrometer (ICP-AES) to be 0.311, 0.542, 0.610, 0.759, 0.812 for the Cu-Pt-1#, Cu-Pt-2#, Cu-Pt-3#, Cu-Pt-4# and Cu-Pt-5#, respectively. The results indicate that the Cu/Pt atomic ratio in the as-synthesized Cu-Pt NCs was directly proportional to the precursors of $\text{Cu}(\text{acac})_2/\text{Pt}(\text{acac})_2$ ratio.

In addition, we investigated the morphology of other Cu-Pt NCs samples with different molar ratio. It shows that all the samples have similar morphology, indicating that the different molar ratio of Cu precursor and Pt precursor has no obvious influence on the morphology of the as-prepared Cu-Pt NCs (Fig. S1a-e). The X-ray diffraction (XRD) peaks of the as-prepared NCs are shown in Fig. S1f. Each diffraction peak is located between the corresponding peaks of pure Pt and Cu, revealing typical characteristics of Cu-Pt alloy NCs. Noteworthy, the peak positions move to the corresponding peak of pure Cu along with the increase of Cu content.

To examine the reduction of dissolved carbon dioxide in the electrolyte solution, cyclic voltammograms (CVs) were recorded in a

typical three-electrode system (Fig. S2). Fig. 2 shows CVs of the Cu-Pt NCs modified electrodes in the absence and presence of CO_2 in 0.5 M KHCO_3 solution. Generally, hydrogen evolution reaction (HER) is a competing process of CO_2 reduction at the electrode. Therefore, it is crucial to suppress hydrogen formation, since it consumes the applied energy instead of the CO_2 reduction. For the Cu-Pt-1# electrode, as shown in Fig. 2a, much higher reduction current was observed for N_2 saturated solution than that for CO_2 saturated solution. It strongly indicates that HER dominated the reduction process and the presence of CO_2 seems to inhibit the HER at potentials lower than -1.1 V. In sharp contrast, all other samples exhibited obvious catalytic activity towards CO_2 reduction. The current density of CO_2 reduction outcompeting HER could be simply calculated by subtracting the current density obtained at the black lines (HER current) from that recorded at the red lines (the overall current of HER and CO_2 reduction), as inferred by the arrow lines in the figures. Noteworthy, we found that the activity of the Cu-Pt NCs should be closely associated with the composition of the NCs. Fig. 2b-d suggest that increasing the Cu content in the Cu-Pt NCs facilitates the reduction of CO_2 , leading to enhanced activity of CO_2 reduction. However, Fig. 2e shows that, for Cu-Pt-5# sample which the Cu : Pt was increased to 5:1, CO_2 reduction was subsequently suppressed. The results clearly indicate that an optimum content of Cu in the NCs is required to achieve maximum activity for CO_2 reduction. To further clarify this point, Table S1 presents the onset potentials obtained with the samples in N_2 and CO_2 saturated conditions. Also, the current density of CO_2 reduction at a potential of -1.3 V (vs. SCE) was calculated and compared in Table S1. Among all the samples, Cu-Pt-4#, which the atomic ratio of Cu : Pt is 3:1, exhibited the best performance for CO_2 reduction, i.e. the lowest onset potential (ca. -0.972 V) and highest CO_2 reduction current density (ca. 0.598 mA cm^{-2} at -1.3 V vs. SCE).

To compare the overall catalytic activities of the samples, linear sweep voltammetry (LSV) was recorded in 0.5 M KHCO_3 electrolyte with a scan rate of 10 mV/s in a potential range from -0.6 to -1.6 V (vs. SCE). The solution was saturated with CO_2 by bubbling CO_2 gas for at least 30 min. Once again, as shown in Fig. S3, the Cu-Pt NCs samples exhibit obviously compositional dependent activities. Notably, Cu-Pt-4# gives the highest current density among all samples. Therefore, it can be concluded that the Cu-Pt NCs with an optimized atomic molar ratio of 3:1 (Cu : Pt) likely possesses the highest activity both for CO_2 reduction and for the overall reduction.

Selectivity of the CO_2 reduction is important for assessing the performance of a catalyst. In order to evaluate this, we used the on-line electrochemical gas chromatograph (GC) technique to detect gas

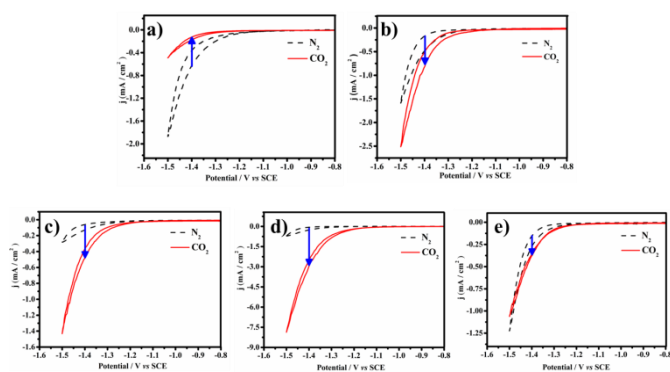


Fig. 2 The cyclic voltammograms of catalysts were recorded in N_2 - and CO_2 -saturated 0.5 M KHCO_3 with a scan rate of 10 mV/s between -0.8 and -1.5 V (vs. SCE). (a) Cu-Pt-1#, (b) Cu-Pt-2#, (c) Cu-Pt-3#, (d) Cu-Pt-4#, (e) Cu-Pt-5#.

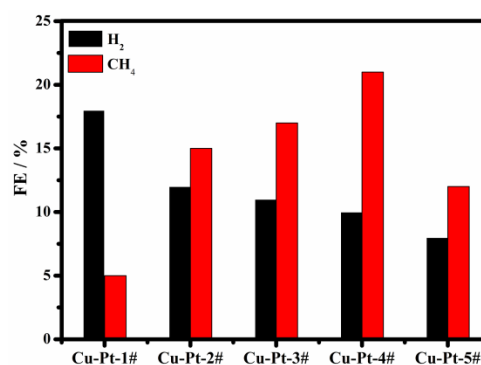


Fig. 3 The faradaic efficiencies of H_2 , CH_4 at different Cu-Pt NCs. $E = -1.6$ V. Electrolyte: 0.5 M KHCO_3 , $\text{pH} = 7.3$.

productions and estimate their faradaic efficiency (FE). As illustrated schematically in Fig. S4, the on-line electrochemical GC setup consists of a CHI 760D electrochemical workstation, home-made H-type electrochemical cell and gas chromatography system. During the electrolysis, the flow of CO₂ atmosphere was maintained and the electrolyte was kept under constant stirring. The GC analysis proves the presence of H₂ and CH₄ as the production of CO₂ electrochemical reduction at Cu-Pt NCs electrode under these conditions. The faradaic efficiency of the products was calculated according to the method as depicted in ESI.^[40] Fig. 3 summarizes the faradaic efficiency of H₂, CH₄ obtained at the Cu-Pt-1#, Cu-Pt-2#, Cu-Pt-3#, Cu-Pt-4# and Cu-Pt-5# electrodes, respectively. The sample of Cu-Pt-4# gives highest faradaic efficiency of CH₄ with a value of 21 %, which is comparable to the results previously reported by C. Buess-Herman et.al.(ca. 20 %), M. Jin et.al.(ca. 38 %) and I. Chorkendorff et.al.(ca. 10 %)^[24,30,41] In addition, we made a comparison between the achieved faradaic efficiency for methane of Cu-Pt NCs and of polycrystalline Cu and Cu nanoparticles. We found that the faradaic efficiency for methane of polycrystalline Cu and Cu nanoparticles was ca. 4 % and 1%, respectively. This observation is in agreement with the previously reported results.^[25] These results indicate that the NCs have advantage for CH₄ production as a promising CO₂ catalyst.

Finally, it is worth understanding the compositional dependent activity of the Cu-Pt NCs that is why the sample of Cu-Pt (3:1) NCs exhibits the highest activity and faradaic efficiency for CO₂ electroreduction. Peterson et al. have reported the DFT calculations, providing useful insights into how copper catalyses CO₂ reduction to CH₄.^[20] The DFT calculation suggests that a key step in the formation of CH₄ from CO₂ reduction is the protonation of adsorbed CO* to form adsorbed HCO* (CO* + H⁺ + e⁻ → HCO*). It means that selectivity-determining step for CO₂ electroreduction on Cu involves the reduction of CO to CHO, which eventually leads to formation of CH₄.^[23] On the other hand, Pt is known as an element with high activity for HER due to its unique affinity for proton.^[42] Thus, the presence of Pt in the NCs should facilitate the protonation of adsorbed CO*. As a result, we assume that a synergistic effect between Cu and Pt should greatly benefit for producing CH₄ by effectively electroreduction of CO₂. Fig. 4 presents a proposed mechanism illustrating the above depicted reaction process. However, a recent study elucidated that Pt in bimetallic catalysts would not be stable during the electrochemical reduction of CO₂. The strong interaction between Pt and CO* would likely cause Pt segregation, therefore facilitating the HER over CO₂ reduction.^[41] Similarly, We found that the Cu-Pt NCs suffer deactivation during the electrochemical reduction of CO₂. We measured the efficiency of the reduction of CO₂ as a function of time, which was shown in Figure S5. The production of methane from CO₂ drops clearly at the beginning, and reaches an efficiency of ~5% after 25 min. This should be related to the surface state of NCs caused by the electrochemical reaction, which more efforts are required to clarify it. For Cu-Pt-1#, as the Pt content is high, the presence of CO₂ in the solution leads to the production of CH₄ in the cost of greatly suppressing H₂ production. Consequently, more adsorbed CO* was generated due to the increase of Cu content in NCs, therefore improving the production of CH₄. Thereby, an optimized atomic ratio of Cu and Pt (ca. 3:1) contributes to the highest activity of the NCs. However, too much higher Cu content subsequently leads to higher density of adsorbed CO*, while consequently lower adsorbed proton. Correspondingly, the overall performance of the NCs should be limited due to low density of adsorbed proton at the catalyst surface. Meanwhile, we noted that a recently reported study on Au-Cu NCs indicated that Au₃Cu NCs should give the highest performance for CO₂ electroreduction.^[30] We suppose that the differ-

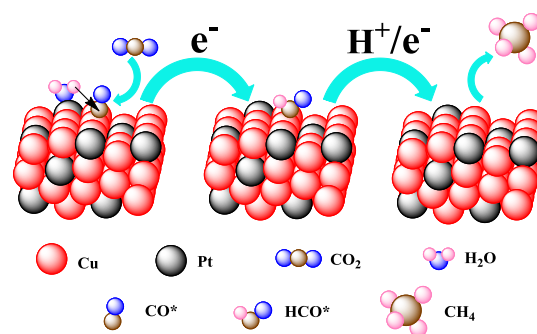


Fig.4 A proposed mechanism illustrating the steps of CO₂ electroreduction and the CH₄ formation occurs at Cu-Pt (3:1) NCs catalyst.

ent optimum atomic ratio of Au : Cu and Pt : Cu might attribute to the different proton affinity of the Pt and Au. In spite that our results should provide experimental evidences for supporting the DFT calculations for Cu-Pt NCs, substantial efforts are still needed to further elucidate clearly the detailed reaction procedure of CO₂ electroreduction on bimetallic NCs.

In summary, we report the preparation of Cu-Pt NCs and investigate its application as electrocatalyst for CO₂ reduction. Uniform sized NCs with concisely controlled atomic ratio were prepared with a simple method. The NCs samples exhibit compositional dependent activities towards CO₂ electroreduction. Among all the as-prepared samples, Cu-Pt (3:1) NCs exhibits the highest activity and faradaic efficiency as an efficient electrocatalyst for CO₂ reduction in 0.5 M KHCO₃ at room temperature. Based on the experimental analysis, we propose a reasonable mechanism to understand the CO₂ electroreduction at the Cu-Pt bimetallic NCs catalyst and illustrate the observed compositional dependent activity of the NCs. This work highlights the importance of compositional effect of NCs on their catalytical activities and provides a strategy for designing efficient catalysts for CO₂ electroreduction in the future.

The authors acknowledge the Chinese Ministry of Science and Technology (2012DFR40240), National Natural Science Foundation of China (Grant nos. 21175012, 21006015 and 21070623), and the Chinese Ministry of Education (Project of New Century Excellent Talents in University) for financial support.

Notes and references

Beijing Key Laboratory for Chemical Power Source and Green Catalysis, School of Chemical Engineering and Environment, Beijing Institute of Technology, Beijing, 100081, China.

Email: bityanyiming@163.com; bitkeningsun@163.com

Electronic Supplementary Information (ESI) available: [Experimental details, Table S1, TEM images of the samples, LSVs, and the testing configuration can be found in the ESI]. See DOI: 10.1039/c000000x/

1 A. Goeppert, M. Czaun, R. B. May, G. K. S. Prakash, G. A. Olah and S. R. Narayanan, *J. Am. Chem. Soc.*, 2011, 133, 20164-20167.

2 G. Centi and S. Perathoner, *Greenhouse Gas Sci Technol.*, 2011, 1, 21-35.

3 Z. Jiang, T. Xiao, V. L. Kuznetsov and P. P. Edwards, *Phil. Trans. R. Soc. A*, 2010, 368, 3343-3364.

4 M. Aresta, A. Dibenedetto and A. Angelini, *Chem. Rev.*, 2014, 114, 1709-1742.

5 D. P. Schrag, *Science*, 2007, 315, 812-813.

- 6 D. T. Whipple and P. J. A. Kenis, *J. Phys. Chem. Lett.*, 2010, 1, 3451-3458.
- 7 D. D. Yuan, C. H. Yan, B. Lu, H. X. Wang, C. M. Zhong and Q. H. Cai, *Electrochim. Acta*, 2009, 54, 2912-2915.
- 8 A. S. Agarwal, Y. M. Zhai, D. Hill and N. Sridhar, *ChemSusChem*, 2011, 4, 1301-1310.
- 9 J. L. Qiao, Y. Y. Liu, F. Hong and J. J. Zhang, *Chem. Soc. Rev.*, 2014, 43, 631-675.
- 10 C. Costentin, M. Robert and J. Savéant, *Chem. Soc. Rev.*, 2013, 42, 2423-2436.
- 11 C. D. Windle and R. N. Perutz, *Coordination Chemistry Reviews*, 2012, 256, 2562-2570.
- 12 A. A. Peterson, J. K. Nørskov, *J. Phys. Chem. Lett.*, 2012, 3, 251-258.
- 13 M. Gattrell, N. Gupta and A. Co, *Journal of Electroanalytical Chemistry*, 2006, 594, 1-19.
- 14 Y. Hori, K. Kikuchi and S. Suzuki, *Chem. Lett.*, 1985, 14, 1695-1698.
- 15 Y. Hori, A. Murata, R. and Takahashi, *J. Chem. Soc. Faraday Trans. 1*, 1989, 85, 2309-2326.
- 16 K. J. P. Schouten, Y. Kwon, C. J. M. van der Ham, Z. Qin and M. T. M. Koper, *Chem. Sci.*, 2011, 2, 1902-1909.
- 17 K. P. Kuhl, E. R. Cave, D. N. Abram and T. F. Jaramillo, *Energy Environ. Sci.*, 2012, 5, 7050-7059.
- 18 Y. Hori, R. Takahashi, Y. Yoshinami and A. Murata, *J. Phys. Chem. B*, 1997, 101, 7075-7081.
- 19 K. J. P. Schouten, Z. S. Qin, E. P. Gallent and M. T. M. Koper, *J. Am. Chem. Soc.*, 2012, 134, 9864-9867.
- 20 A. A. Peterson, F. Abild-Pedersen, F. Studt, J. Rossmeisl and J. K. Nørskov, *Energy Environ. Sci.*, 2010, 3, 1311-1315.
- 21 W. J. Durand, A. A. Peterson, F. Studt, F. Abild-Pedersen and J. K. Nørskov, *Surf. Sci.*, 2011, 605, 1354-1359.
- 22 P. Hirunsit, *J. Phys. Chem. C*, 2013, 117, 8262-8268.
- 23 X. Nie, M. R. Esopi, M. J. Janik, and A. Asthagiri, *Angew. Chem.*, 2013, 125, 2519-2522.
- 24 J. Christophe, Th. Doneux and C. Buess-Herman, *Electrocatal*, 2012, 3, 139-146.
- 25 W. Tang, A. A. Peterson, A. S. Varela, Z. P. Jovanov, L. Bech, W. J. Durand, S. Dahl, J. K. Nørskov, I. Chorkendorff, *Phys. Chem. Chem. Phys.*, 2012, 14, 76-81.
- 26 C. W. Li and M. W. Kanan, *J. Am. Chem. Soc.*, 2012, 134, 7231-7234.
- 27 R. Reske, M. Duca, M. Oezaslan, K. J. P. Schouten, M. T. M. Koper and P. Strasser, *J. Phys. Chem. Lett.*, 2013, 4, 2410-2413.
- 28 L. Chen, C. Bock, P. H. J. Mercier and B. R. MacDougall, *Electrochimica Acta*, 2012, 77, 212-224.
- 29 Z. Xu, E. Lai, Y. Shao-Horn and K. Hamad-Schifferli, *Chem. Commun.*, 2012, 48, 5626-5628.
- 30 W. Zhao, L. Yang, Y. Yin and M. Jin, *J. Mater. Chem. A*, 2014, 2, 902-906.
- 31 S. Tominaka, M. Shigeto, H. Nishizeko and T. Osaka, *Chem. Commun.*, 2010, 46, 8989-8991.
- 32 H. Yang, L. Dai, D. Xu, J. Fang, S. Zou, *Electrochimica Acta*, 2010, 55, 8000-8004.
- 33 Z. Zhang, Y. Yang, F. Nosheen, P. Wang, J. Zhang, J. Zhuang and X. Wang, *Small*, 2013, 9, 3063-3069.
- 34 D. Xu, Z. Liu, H. Yang, Q. Liu, J. Zhang, J. Fang, S. Zou and K. Sun, *Angew. Chem. Int. Ed.*, 2009, 48, 4217-4221.
- 35 B.Y. Xia, H. B. Wu, X. Wang and X. W. Lou, *J. Am. Chem. Soc.*, 2012, 134, 13934-13937.
- 36 S. Zhou, B. Varughese, B. Eichhorn, G. Jackson and K. McIlwrath, *Angew. Chem.*, 2005, 117, 4615-4619.
- 37 T. Komatsu, M. Takasaki, K. Ozawa, S. Furukawa and A. Muramatsu, *J. Phys. Chem. C*, 2013, 117, 10483-10491.
- 38 D. Wang, Y. Yu, H. L. Xin, R. Hovden, P. Ercius, J. A. Mundy, H. Chen, J. H. Richard, D. A. Muller, F. J. DiSalvo and H. D. Abruña, *Nano Lett.*, 2012, 12, 5230-5238.
- 39 C. Güneçci, D. U. Cearnaigh, D. J. Casadonte, Jr. and Carol Korzeniewski, *J. Mater. Chem. A*, 2013, 1, 2322-2330.
- 40 W. Zhu, R. Michalsky, Ö. Metin, H. Lv, S. Guo, C. J. Wright, X. Sun, A. A. Peterson and S. Sun, *J. Am. Chem. Soc.*, 2013, 135, 16833-16836.
- 41 A. S. Varela, C. Schlaup, Z. P. Jovanov, P. Malacrida, S. Horch, I. E. L. Stephens and I. Chorkendorff, *J. Phys. Chem. C*, 2013, 117, 20500-20508.
- 42 M. Nakamura, T. Kobayashi and N. Hoshi, *Surf. Sci.*, 2011, 605, 1462-1465.